Analytical and Numerical Solutions for Nonlinear Equations
©Available online at https://ansne.du.ac.ir/
Online ISSN: 3060–785X
2027, Volume 12, Issue 1, pp. 191–210
Research article

A Fully Discrete Bernstein Collocation Scheme for Distributed-Order Fractional Diffusion Equations with Bessel and Riesz Derivatives

Ali Mankhi Jebur Alaayedi[1], Safar Irandoust-Pakchin[1], Mohammad Hossein Derakhshan[1,*]

[1] Department of Applied Mathematics, Faculty of Mathematics, Statistics and Computer Sciences, University of Tabriz, Tabriz, Iran

* **Corresponding author(s):** m.h.derakhshan.20@gmail.com

Received: 28/08/2026 **Revised:** 07/10/2026 **Accepted:** 18/10/2026 **Published:** 02/11/2026 10.22128/ansne.2026.3442.1238

Abstract

In this study, we propose a distributed-order fractional diffusion model that incorporates a Bessel-type fractional derivative in time and a Riesz fractional derivative in space, providing a versatile framework to describe complex diffusion processes exhibiting both memory effects and nonlocal interactions. To numerically solve the proposed model, we develop a fully discrete scheme combining the Bernstein polynomial collocation method for the temporal distributed-order derivative with a finite difference approximation for the spatial Riesz derivative. The temporal approximation ensures high-order accuracy and efficient evaluation of the distributed-order operator, while the spatial discretization captures the nonlocal behavior of the Riesz derivative. A rigorous theoretical analysis of the scheme is carried out, establishing unconditional stability and second-order convergence in both time and space. Numerical simulations validate the theoretical results, demonstrating that the method accurately captures the dynamics of the distributed-order fractional diffusion process and achieves the expected convergence rates. The proposed framework offers a powerful and reliable tool for modeling and simulating complex diffusion phenomena, and it can be further extended to multi-dimensional and variable-order settings for broader applications in physics, engineering, and applied sciences.

Keywords: Distributed-order, Fractional diffusion, Bernstein polynomials, Riesz derivative, Bessel operator, Numerical simulation.

Mathematics Subject Classification (2020): 26A33, 35R11, 65M70, 65M06, 35K05, 65M12

1 Introduction

The distributed-order (DO) fractional operator is a powerful and generalized mathematical tool that extends the concept of classical derivatives to fractional orders, allowing the inclusion of multiple derivative orders within a single operator [19, 27, 28]. Unlike standard integer-order derivatives, which only capture local rates of change, the DO fractional operator can describe processes where the current state depends on the entire history of the system. Mathematically, it is expressed as an integral over a continuum of derivative orders weighted by a non-negative function, which characterizes the relative contribution of each order. This general formulation not only encompasses many classical and single-order fractional derivatives as special cases but also provides the flexibility to tailor the operator to the specific memory or hereditary characteristics of the physical system under consideration. Physically, the DO operator is particularly relevant for modeling complex diffusion processes, viscoelastic materials, heat conduction in heterogeneous media, and transport phenomena in porous

COPYRIGHTS: ©2027, Analytical and Numerical Solutions for Nonlinear Equations published by Damghan University.
This is an open access article published under the *CC BY 4 DEED* license

or fractal-like structures. It captures memory effects, anomalous diffusion, and nonlocal interactions, which cannot be adequately described using integer-order models. In engineering, it is used to model materials with time-dependent stress-strain relationships, control systems with history-dependent responses, and viscoelastic damping in structures. In physics, applications include anomalous transport in plasma, subdiffusion in biological tissues, and wave propagation in complex media. Over the last few decades, considerable attention has been devoted to the formulation, analysis, and numerical solution of distributed-order fractional differential equations due to their ability to accurately model such complex phenomena. Analytical methods, including Laplace and Fourier transform techniques, have been employed to study the behavior of these equations under various boundary and initial conditions, while numerical approaches such as finite difference, finite element, and spectral methodshave been developed to provide efficient and accurate approximations for practical simulations. Overall, the distributed-order fractional operator provides a versatile framework that bridges theoretical analysis and real-world modeling, enabling researchers and engineers to capture and simulate the rich dynamical behaviors of systems with memory, heterogeneity, and long-range interactions.

The general form of these equations is defined through a DO fractional operator, expressed as

$$\mathscr{D} = \int_a^b \psi(\beta)\, \mathbf{D}^{(\beta)}\, d\beta, \tag{1}$$

where $\mathbf{D}^{(\beta)}$ denotes a chosen fractional derivative of order β, and $\psi(\beta)$ represents an appropriate weighting function that characterizes the distribution of derivative orders over the interval $[a,b]$. This operator provides a unified framework encompassing numerous conventional and fractional derivatives as special instances, depending on the specific form of $\psi(\beta)$.

For example, consider a generalized form of the classical Euler-Poisson-Darboux equation, which is a type of hyperbolic partial differential equation, written as

$$\left[\frac{\partial^2}{\partial t^2} + \frac{\delta}{t}\frac{\partial}{\partial t}\right] u(\mathbf{y}_n,t) = u_{y_1y_1} + u_{y_2y_2} + \cdots + u_{y_ny_n}, \quad (\mathbf{y}_n = y_1, y_2, \ldots, y_n) \in \mathbb{R}^n, \quad t > 0, \quad \delta > 0. \tag{2}$$

This operator can be generalized in terms of a fractional Bessel-type derivative, and various results have been obtained for its solution using integral transform techniques [22–24]. Further studies on different boundary conditions and domains, as well as the physical and mathematical behavior of the classical wave equation, can be found in [4, 5].

Inspired by the concept of distributed-order derivatives, we define the generalized DO Bessel fractional operator as

$$\mathscr{B}_t^{\phi(\beta)} = \int_p^q \phi(\beta) \left[\frac{\partial^2}{\partial t^2} + \frac{\delta}{t}\frac{\partial}{\partial t}\right]^{\beta} d\beta, \tag{3}$$

which allows us to reformulate the hyperbolic equation in a distributed-order fractional sense. Using this operator, we consider the following distributed-order (DO) fractional diffusion equation:

$$\mathscr{B}_t^{\phi(\beta)} u(y,t) = D_\eta \frac{\partial^\eta u(y,t)}{\partial |y|^\eta} + g(y,t), \qquad D_\eta > 0, \quad 0 < y < L, \quad 0 < t < T, \tag{4}$$

where $\mathscr{B}_t^{\phi(\beta)} u(y,t)$ denotes the distributed-order time-fractional derivative of Bessel type, defined by

$$\mathscr{B}_t^{\phi(\beta)} u(y,t) = \int_0^1 B^{\beta}_{\delta,0^+}\, u(y,t)\, \phi(\beta)\, d\beta, \tag{5}$$

with $\phi(\beta)$ being a continuous, nonnegative weight function satisfying

$$\int_0^1 \phi(\beta)\, d\beta = W > 0, \qquad \phi(\beta) \geq 0, \quad \beta \in [0,1]. \tag{6}$$

In this formulation, the temporal evolution is governed by a distributed-order fractional derivative of Bessel type, while the spatial nonlocality is characterized by a Riesz fractional derivative of order $\eta \in (0,2]$. The Riesz fractional derivative in one-dimensional finite domain $(0,L)$ is defined in terms of the left- and right-sided Riemann–Liouville fractional derivatives as follows [8]:

$$\frac{\partial^\eta u(y,t)}{\partial |y|^\eta} = -\frac{1}{2\cos(\frac{\pi\eta}{2})} \left({}_0D_y^\eta u(y,t) + {}_yD_L^\eta u(y,t)\right), \qquad 0 < y < L, \tag{7}$$

where ${}_0D_y^\eta$ and ${}_yD_L^\eta$ denote the left- and right-sided Riemann–Liouville fractional derivatives, respectively, defined by

$$ {}_0D_y^\eta u(y,t) = \frac{1}{\Gamma(n-\eta)} \frac{d^n}{dy^n} \int_0^y \frac{u(\xi,t)}{(y-\xi)^{\eta-n+1}} \, d\xi, \qquad n-1 < \eta < n, \tag{8} $$

$$ {}_yD_L^\eta u(y,t) = \frac{(-1)^n}{\Gamma(n-\eta)} \frac{d^n}{dy^n} \int_y^L \frac{u(\xi,t)}{(\xi-y)^{\eta-n+1}} \, d\xi, \qquad n-1 < \eta < n. \tag{9} $$

The Riesz operator (7) represents a symmetric combination of these fractional derivatives and describes nonlocal spatial interactions with power-law decay. This definition ensures that the fractional Laplacian in a finite spatial interval $(0,L)$ is properly approximated through Riemann–Liouville operators, preserving the boundary dependence of the problem.

The distributed-order fractional diffusion model considered in this study is important because it generalizes classical diffusion equations by incorporating multiple fractional orders, allowing it to capture complex memory effects and hereditary properties observed in many physical systems. Fractional derivatives provide a natural framework to describe anomalous diffusion, which occurs in heterogeneous and porous media, viscoelastic materials, and biological tissues. The Bessel-type time derivative models temporal dynamics with singularities at the initial time, reflecting processes with strong memory near $t = 0$. The Riesz fractional derivative captures long-range spatial interactions, which are essential for describing nonlocal transport phenomena. Studying this model numerically allows for accurate simulation of processes where classical integer-order derivatives fail to reproduce experimental observations. Applications of such models include subsurface pollutant transport, diffusion in complex materials, and wave propagation in heterogeneous media. Overall, the proposed distributed-order framework provides both theoretical insight and practical tools for modeling a wide range of real-world phenomena exhibiting anomalous diffusion.

The novelty of the present work lies in the combination of the distributed-order Bessel fractional derivative in time with the Riesz fractional derivative in space, providing a flexible and accurate framework for modeling complex diffusion processes. Unlike classical approaches, the distributed-order formulation allows the simultaneous representation of multiple memory effects, which is essential for capturing anomalous dynamics in heterogeneous media. The use of Bernstein polynomials for temporal discretization is advantageous because it offers high-order accuracy, smooth approximations, and a simple collocation-based matrix formulation. This method enables an efficient and stable evaluation of the distributed-order fractional operator without resorting to cumbersome integral approximations. In space, the Riesz fractional derivative is approximated using finite difference schemes, which are easy to implement and preserve the nonlocal characteristics of the diffusion process. By combining these approximations, a fully discrete numerical scheme is constructed that is second-order accurate in both time and space. The proposed approach ensures computational efficiency while maintaining rigorous convergence and stability properties. Overall, this method provides a reliable and practical tool for simulating distributed-order fractional diffusion phenomena in applied sciences and engineering.

Numerical methods play a crucial role in the study of fractional differential equations due to the complexity and nonlocal nature of fractional operators. While analytical solutions provide exact expressions for the behavior of mathematical models, they are often limited to simple or idealized cases. In many practical applications, such as modeling diffusion processes, viscoelastic materials, or nonlinear wave propagation, finding a closed-form analytical solution is either extremely difficult or impossible. Therefore, numerical methods offer a practical alternative for obtaining approximate solutions with controllable accuracy [10, 16–18, 21]. One of the main advantages of numerical methods is their flexibility in handling complex boundary conditions, variable coefficients, and fractional orders that are not easily manageable analytically [2, 9, 25]. Moreover, numerical schemes allow researchers to simulate dynamic behavior over time and space, which is essential for understanding phenomena in fractional-order systems [11, 15, 20]. Recent advances have introduced various efficient numerical techniques for solving fractional differential equations, including methods based on Bernstein polynomials [16, 17, 21], wavelet-based approaches [25], Ritz-Piecewise Gegenbauer techniques [9], multiplicative integration strategies [2], and hybrid schemes for multi-dimensional problems [11, 15]. These methods provide significant computational efficiency and high accuracy, making them suitable for practical engineering and physical applications. Numerical approaches also enable the treatment of distributed-order and Bessel-type fractional differential equations, which are highly challenging analytically [1, 3, 7, 12, 20]. Furthermore, these methods facilitate stability analysis, error estimation, and convergence studies, which are often infeasible in purely analytical frameworks [6, 14, 26]. In summary, numerical methods are indispensable in the study of fractional differential equations. They extend the applicability of mathematical models to realistic and complex scenarios where analytical solutions are unattainable, provide tools for precise simulations, and allow for rigorous analysis of stability and convergence. The development and study of numerical techniques are therefore essential for both theoretical

investigations and practical implementations in science and engineering [2, 10, 15, 18, 25].

The remainder of this paper is organized as follows. In Section 2, we present several basic concepts and essential mathematical tools that will be utilized throughout the paper. These preliminaries provide the theoretical foundation necessary for the development of the proposed numerical framework. Section 3 is devoted to a brief review of the definition and fundamental analytical properties of the Bernstein polynomials, which play a crucial role in approximation theory, numerical analysis, and the construction of various spectral and collocation schemes. Their desirable characteristics, such as positivity, smoothness, and the ability to approximate continuous functions with high accuracy, make them particularly suitable for solving fractional differential equations. In Section 4, we apply the Bernstein polynomial basis to construct a time-approximation scheme for the proposed fractional model. This approach allows for efficient temporal discretization while maintaining computational accuracy and stability. Section 5 focuses on the spatial discretization of the problem using finite difference methods for the Riesz fractional derivative. This combination of polynomial approximation in time and finite difference approximation in space provides a flexible and accurate framework for the numerical solution of multi-dimensional fractional problems. The convergence analysis of the fully discrete numerical scheme is presented in Section 6. In this section, we rigorously demonstrate that the proposed algorithm converges to the exact solution under reasonable regularity assumptions. Section 7 is devoted to the stability analysis of the fully discrete scheme. By employing suitable mathematical tools, we establish sufficient conditions ensuring the stability and reliability of the numerical results. Section 8 presents several numerical simulations that illustrate the accuracy, efficiency, and robustness of the proposed numerical method. The obtained results confirm the theoretical predictions and demonstrate the effectiveness of the method in handling various types of fractional models. Finally, Section 9 concludes the paper with a summary of the main findings and discusses possible directions for future research related to the extension of the proposed scheme to more general classes of fractional differential equations.

2 Preliminaries

In this section, we present several basic concepts and mathematical tools that will be used throughout this paper. We first recall the definition of the Gaussian hypergeometric function, followed by the notion of the Bessel fractional integral and derivative operators, which play a fundamental role in the analysis of distributed-order fractional equations. We then derive some useful properties and identities associated with these operators that will be applied in subsequent sections.

Definition 1. *The Gaussian hypergeometric function ${}_2F_1(a,b;c;z)$ is defined as [13, p. 1005, Eq. (9.100)]:*

$$ {}_2F_1(a,b;c;z) = \sum_{k=0}^{\infty} \frac{(a)_k (b)_k}{(c)_k} \frac{z^k}{k!}, \tag{10} $$

where a,b,c are positive parameters, and $(\cdot)_k$ denotes the Pochhammer symbol.

Definition 2 ([22, 23]). *Let $f \in L[0,\infty)$ and suppose that $B^{-(n-\beta)}_{\delta,0^+} \in C^{2n}[0,\infty)$. Then, the left-sided Bessel fractional derivative of order β is defined by*

$$ \begin{aligned} (B^{\beta}_{\delta,0^+} f)(t) &= B^{-(n-\beta)}_{\delta,0^+} B^{n}_{\delta,0^+} f(t) \\ &= \frac{1}{\Gamma(2(n-\beta))} \int_0^t \left(\frac{\xi}{t}\right)^{\delta} \left(\frac{t^2-\xi^2}{2t}\right)^{2(n-\beta)-1} {}_2F_1\left(n-\beta+\frac{\delta-1}{2}, n-\beta; 2(n-\beta); 1-\frac{\xi^2}{t^2}\right) \left[\frac{d^2}{d\xi^2} + \frac{\delta}{\xi}\frac{d}{d\xi}\right]^n f(\xi)\, d\xi, \end{aligned} \tag{11} $$

where $n-1 < \beta < n$ and $n \in \mathbb{N}$.

Example 1. [22, Proposition 5.1] The left-sided Bessel fractional integral of the power function t^m, $m \in \mathbb{R}$, is given by

$$ \left(B^{-\beta}_{\delta,0^+} t^m\right)(t) = 2^{-2\beta} t^{m+2\beta} \frac{\Gamma\left(\frac{m+\delta+1}{2}\right)\Gamma\left(\frac{m}{2}+1\right)}{\Gamma\left(\beta+\frac{m}{2}+1\right)\Gamma\left(\beta+\frac{m+\delta+1}{2}\right)}. \tag{12} $$

Example 2. For $0 < \beta < 1$, and using Example 1, the left-sided Bessel fractional derivative of the power function t^m ($m \in \mathbb{R}$) is obtained

as follows:

$$\begin{aligned}
(B^{\beta}_{\delta,0^+}t^m)(t) &= \frac{1}{\Gamma(2-2\beta)}\int_0^t \left(\frac{\xi}{t}\right)^{\delta}\left(\frac{t^2-\xi^2}{2t}\right)^{1-2\beta} {}_2F_1\left(1-\beta+\frac{\delta-1}{2},1-\beta;2-2\beta;1-\frac{\xi^2}{t^2}\right)\left[\frac{d^2}{d\xi^2}+\frac{\delta}{\xi}\frac{d}{d\xi}\right]\xi^m d\xi \\
&= (m^2-m+m\delta)\frac{1}{\Gamma(2-2\beta)}\int_0^t \left(\frac{\xi}{t}\right)^{\delta}\left(\frac{t^2-\xi^2}{2t}\right)^{1-2\beta} {}_2F_1\left(1-\beta+\frac{\delta-1}{2},1-\beta;2-2\beta;1-\frac{\xi^2}{t^2}\right)\xi^{m-2}d\xi \\
&= (m^2-m+m\delta)\left(B^{-(1-\beta)}_{\delta,0^+}t^{m-2}\right)(t) \\
&= (m^2-m+m\delta)\,2^{-2+2\beta}t^{m-2\beta}\frac{\Gamma\left(\frac{m+\delta-1}{2}\right)\Gamma\left(\frac{m}{2}\right)}{\Gamma\left(\frac{m}{2}-\beta+1\right)\Gamma\left(\frac{m+\delta+1}{2}-\beta\right)}.
\end{aligned} \tag{13}$$

3 Bernstein Polynomials and Their Properties

In this section, we review the definition and main analytical properties of the Bernstein polynomials, which are widely used in approximation theory, numerical analysis, and the construction of spectral and collocation methods. These polynomials form a complete and linearly independent basis on the unit interval $[0,1]$ and possess several useful properties such as nonnegativity, partition of unity, and endpoint interpolation. Furthermore, we discuss their orthogonality conditions and related integral identities that will be employed in later sections.

Definition 3. *For a nonnegative integer n and $i = 0,1,2,\ldots,n$, the Bernstein polynomial of degree n and order i is defined on the interval $[0,1]$ by*

$$B_{i,n}(x) = \binom{n}{i}x^i(1-x)^{n-i}, \qquad x \in [0,1]. \tag{14}$$

Here, $\binom{n}{i} = \frac{n!}{i!(n-i)!}$ denotes the binomial coefficient.

The Bernstein basis functions $\{B_{i,n}(x)\}_{i=0}^n$ possess several fundamental analytical properties that make them particularly suitable for approximation and numerical analysis. First, they are *nonnegative* over the interval $[0,1]$, i.e.,

$$B_{i,n}(x) \geq 0, \qquad \forall x \in [0,1],\ i = 0,1,\ldots,n. \tag{15}$$

Moreover, they form a partition of unity, ensuring that their sum at any point in the interval is equal to one:

$$\sum_{i=0}^{n} B_{i,n}(x) = 1, \qquad \forall x \in [0,1]. \tag{16}$$

At the endpoints of the domain, the Bernstein polynomials satisfy the *endpoint interpolation property*, given by

$$B_{0,n}(0) = 1, \quad B_{n,n}(1) = 1, \qquad B_{i,n}(0) = B_{i,n}(1) = 0 \quad \text{for } i \neq 0,n. \tag{17}$$

In addition, the Bernstein polynomials exhibit a symmetry property with respect to the midpoint of the interval, expressed as

$$B_{i,n}(x) = B_{n-i,n}(1-x). \tag{18}$$

These fundamental characteristics nonnegativity, unity partition, endpoint interpolation, and symmetryconstitute the core features that enable Bernstein polynomials to serve as a stable and shape preserving basis for polynomial approximation on the interval $[0,1]$. Bernstein polynomials satisfy a simple recursive relation that facilitates numerical computation:

$$B_{i,n}(x) = (1-x)B_{i,n-1}(x) + xB_{i-1,n-1}(x), \tag{19}$$

where $B_{i,n-1}(x) = 0$ if $i < 0$ or $i > n-1$. The first derivative of $B_{i,n}(x)$ can be expressed as a linear combination of Bernstein polynomials of lower degree:

$$\frac{d}{dx}B_{i,n}(x) = n\left[B_{i-1,n-1}(x) - B_{i,n-1}(x)\right]. \tag{20}$$

Similarly, the integral of $B_{i,n}(x)$ over the unit interval is given by

$$\int_0^1 B_{i,n}(x)\,dx = \frac{1}{n+1}. \tag{21}$$

More generally, for $i, j = 0, 1, \ldots, n$, one has

$$\int_0^1 B_{i,n}(x)B_{j,n}(x)\,dx = \frac{\binom{n}{i}\binom{n}{j}}{\binom{2n}{i+j}}\frac{1}{2n+1}. \tag{22}$$

Although Bernstein polynomials are not orthogonal in the standard $L^2[0,1]$ inner product, they satisfy a weighted orthogonality condition under a suitable Beta-type weight function. Let $w(x) = x^\alpha(1-x)^\beta$ with $\alpha, \beta > -1$. Then the inner product

$$\langle B_{i,n}, B_{j,n}\rangle_w = \int_0^1 B_{i,n}(x)B_{j,n}(x)w(x)\,dx \tag{23}$$

can be evaluated explicitly as

$$\langle B_{i,n}, B_{j,n}\rangle_w = \binom{n}{i}\binom{n}{j}\mathrm{B}(i+j+\alpha+1, 2n-i-j+\beta+1), \tag{24}$$

where $\mathrm{B}(\cdot,\cdot)$ is the Beta function defined by

$$\mathrm{B}(p,q) = \int_0^1 t^{p-1}(1-t)^{q-1}dt = \frac{\Gamma(p)\Gamma(q)}{\Gamma(p+q)}. \tag{25}$$

In the special case $\alpha = \beta = 0$, the inner product reduces to

$$\langle B_{i,n}, B_{j,n}\rangle = \frac{\binom{n}{i}\binom{n}{j}}{\binom{2n}{i+j}}\frac{1}{2n+1}, \tag{26}$$

which implies that the Bernstein basis functions are linearly independent and span the space of all polynomials of degree at most n. A fundamental property of Bernstein polynomials is their role in the Bernstein approximation theorem. For any continuous function $f \in C[0,1]$, the Bernstein polynomial of degree n associated with f is defined as

$$B_n(f;x) = \sum_{i=0}^{n} f\left(\frac{i}{n}\right) B_{i,n}(x), \tag{27}$$

and it holds that

$$\lim_{n\to\infty} B_n(f;x) = f(x), \qquad \text{uniformly for } x \in [0,1]. \tag{28}$$

This theorem guarantees that any continuous function on $[0,1]$ can be uniformly approximated by a sequence of Bernstein polynomials.

4 Time Approximation of the Proposed Model using Bernstein Polynomials

In this section, we construct an approximation of the distributed-order (DO) diffusion model

$$\mathscr{B}_t^{\phi(\beta)}u(y,t) = D_\eta \frac{\partial^\eta u(y,t)}{\partial|y|^\eta} + g(y,t), \qquad D_\eta > 0, \quad 0 < y < L, \quad 0 < t < T, \tag{29}$$

in the direction of the time variable only, using the Bernstein polynomial basis defined in (14). The spatial derivative remains in its continuous form, and our focus is solely on the time discretization of the fractional operator. Let the time domain $[0,T]$ be normalized to $[0,1]$ via the transformation

$$\tau = \frac{t}{T}, \qquad 0 \le \tau \le 1. \tag{30}$$

We approximate the temporal dependence of $u(y,t)$ at a fixed spatial point y by a finite Bernstein series of degree n:

$$u(y,t) \approx U_n(y,\tau) = \sum_{i=0}^{n} a_i(y)\,B_{i,n}(\tau), \tag{31}$$

where the Bernstein basis functions are given by

$$B_{i,n}(\tau) = \binom{n}{i} \tau^i (1-\tau)^{n-i}, \qquad i = 0,1,\ldots,n. \tag{32}$$

The coefficients $a_i(y)$ represent the approximate nodal values of $u(y,t)$ in time, and will be determined later by collocation or projection methods. Recall that the time-fractional distributed-order Bessel derivative is defined as

$$\mathscr{B}_t^{\phi(\beta)} u(y,t) = \int_0^1 B^{\beta}_{\delta,0^+} u(y,t)\, \phi(\beta)\, d\beta, \tag{33}$$

where $B^{\beta}_{\delta,0^+}$ denotes the left-sided Bessel fractional derivative of order β. Substituting the Bernstein approximation (31) into (33) gives

$$\mathscr{B}_t^{\phi(\beta)} u(y,t) \approx \int_0^1 \left[\sum_{i=0}^{n} a_i(y)\, B^{\beta}_{\delta,0^+} B_{i,n}(\tau) \right] \phi(\beta)\, d\beta. \tag{34}$$

Each Bernstein basis function $B_{i,n}(\tau)$ is a polynomial of degree n. Expanding it explicitly and using the linearity of $B^{\beta}_{\delta,0^+}$, we have

$$B^{\beta}_{\delta,0^+} B_{i,n}(\tau) = \binom{n}{i} \sum_{k=0}^{n-i} (-1)^k \binom{n-i}{k} B^{\beta}_{\delta,0^+} \tau^{i+k}. \tag{35}$$

According to the formula (13), the Bessel fractional derivative of a power function is expressed as

$$B^{\beta}_{\delta,0^+} \tau^m = C(m,\beta,\delta)\, \tau^{m-2\beta}, \tag{36}$$

where the coefficient $C(m,\beta,\delta)$ is given explicitly by

$$C(m,\beta,\delta) = 2^{-2(1-\beta)} (m^2 - m + m\delta) \frac{\Gamma\left(\frac{m+\delta-1}{2}\right) \Gamma\left(\frac{m}{2}\right)}{\Gamma\left(\frac{m}{2} - \beta + 1\right) \Gamma\left(\frac{m+\delta+1}{2} - \beta\right)}. \tag{37}$$

Substituting (36) into (35), we obtain

$$B^{\beta}_{\delta,0^+} B_{i,n}(\tau) = \binom{n}{i} \sum_{k=0}^{n-i} (-1)^k \binom{n-i}{k} C(i+k,\beta,\delta)\, \tau^{i+k-2\beta}. \tag{38}$$

The distributed-order integral in β is approximated by an M-point quadrature:

$$\int_0^1 (\cdot)\, \phi(\beta)\, d\beta \approx \sum_{q=1}^{M} \omega_q\, (\cdot)\big|_{\beta=\beta_q}, \tag{39}$$

where $\omega_q = w_q\, \phi(\beta_q)$ are the composite weights. Applying (39) to (34) yields

$$\mathscr{B}_t^{\phi(\beta)} u(y,t) \approx \sum_{q=1}^{M} \omega_q \sum_{i=0}^{n} a_i(y)\, B^{\beta_q}_{\delta,0^+} B_{i,n}(\tau), \tag{40}$$

where $B^{\beta_q}_{\delta,0^+} B_{i,n}(\tau)$ is given explicitly by (38). For computational implementation, it is convenient to express the time-fractional distributed-order operator in a discrete matrix form. Let us define the Bernstein derivative matrix associated with the Bessel fractional operator of order β_q as

$$\left[\mathbf{D}_B^{(\beta_q)}\right]_{r,i} = B^{\beta_q}_{\delta,0^+} B_{i,n}(\tau_r)\Big|_{\tau_r = \frac{r}{n}}, \qquad r,i = 0,1,\ldots,n, \tag{41}$$

where $\tau_r = \frac{r}{n}$ are the collocation points in the normalized time domain $[0,1]$. Thus, for a fixed β_q, the action of the Bessel fractional operator on the Bernstein expansion coefficients can be written in compact matrix-vector form as

$$\mathbf{D}_B^{(\beta_q)}\, \mathbf{a}(y) = \begin{bmatrix} B^{\beta_q}_{\delta,0^+} B_{0,n}(\tau_0) & \cdots & B^{\beta_q}_{\delta,0^+} B_{n,n}(\tau_0) \\ \vdots & \ddots & \vdots \\ B^{\beta_q}_{\delta,0^+} B_{0,n}(\tau_n) & \cdots & B^{\beta_q}_{\delta,0^+} B_{n,n}(\tau_n) \end{bmatrix} \begin{bmatrix} a_0(y) \\ a_1(y) \\ \vdots \\ a_n(y) \end{bmatrix} = \begin{bmatrix} \sum_{i=0}^{n} a_i(y)\, B^{\beta_q}_{\delta,0^+} B_{i,n}(\tau_0) \\ \sum_{i=0}^{n} a_i(y)\, B^{\beta_q}_{\delta,0^+} B_{i,n}(\tau_1) \\ \vdots \\ \sum_{i=0}^{n} a_i(y)\, B^{\beta_q}_{\delta,0^+} B_{i,n}(\tau_n) \end{bmatrix}. \tag{42}$$

Equation (42) shows that each row of the matrix $\mathbf{D}_B^{(\beta_q)}$ corresponds to the evaluation of the fractional derivative of all Bernstein basis functions at a given collocation point τ_r. Then, the distributed-order (DO) time operator at these collocation points can be expressed as the weighted sum over the discrete fractional orders:

$$\mathscr{B}_t^{\phi(\beta)}\mathbf{u}(y) \approx \sum_{q=1}^{M} \omega_q \mathbf{D}_B^{(\beta_q)} \mathbf{a}(y), \tag{43}$$

where

$$\mathbf{u}(y) = [u(y,\tau_0), u(y,\tau_1), \ldots, u(y,\tau_n)]^T, \qquad \mathbf{a}(y) = [a_0(y), a_1(y), \ldots, a_n(y)]^T.$$

Substituting the Bernstein approximation (43) into the main model equation (29), we obtain the semi-discrete form of the proposed model (discrete in time and continuous in space):

$$\sum_{q=1}^{M} \omega_q \mathbf{D}_B^{(\beta_q)} \mathbf{a}(y) = D_\eta \frac{\partial^\eta \mathbf{u}(y)}{\partial |y|^\eta} + \mathbf{g}(y), \tag{44}$$

where

$$\mathbf{g}(y) = [g(y,\tau_0), g(y,\tau_1), \ldots, g(y,\tau_n)]^T.$$

The matrix relation (44) constitutes the time-discretized form of the distributed-order diffusion equation using the Bernstein polynomial approximation. It explicitly reveals how the distributed-order Bessel fractional derivative acts through a weighted combination of the Bernstein derivative matrices $\mathbf{D}_B^{(\beta_q)}$.

5 Spatial Discretization using Finite Differences for the Riesz Fractional Derivative

In this section, we describe a detailed spatial discretization for the Riesz fractional derivative $\frac{\partial^\eta u(y,t)}{\partial |y|^\eta}$ using finite difference approximations. Combined with the time-direction Bernstein polynomial approximation, this leads to a fully discrete numerical scheme for the distributed-order diffusion equation. Let the spatial interval $[0,L]$ be uniformly discretized into N subintervals of size

$$h = \frac{L}{N}, \quad y_j = jh, \quad j = 0,1,\ldots,N. \tag{45}$$

We define the discrete solution vector at time collocation point τ_r as

$$\mathbf{u}^r = \begin{bmatrix} u_0^r \\ u_1^r \\ \vdots \\ u_N^r \end{bmatrix} \approx \begin{bmatrix} u(y_0,\tau_r) \\ u(y_1,\tau_r) \\ \vdots \\ u(y_N,\tau_r) \end{bmatrix}. \tag{46}$$

The Riesz fractional derivative of order $0 < \eta \leq 2$ can be expressed in terms of the left- and right-sided Riemann-Liouville derivatives:

$$\frac{\partial^\eta u(y,t)}{\partial |y|^\eta} = -\frac{1}{2\cos(\pi\eta/2)} \left({}_0D_y^\eta u(y,t) + {}_yD_L^\eta u(y,t) \right), \tag{47}$$

where

$${}_0D_y^\eta u(y,t) = \frac{1}{\Gamma(m-\eta)} \frac{d^m}{dy^m} \int_0^y \frac{u(\xi,t)}{(y-\xi)^{\eta-m+1}} d\xi, \qquad m = \lceil \eta \rceil,$$

$${}_yD_L^\eta u(y,t) = \frac{(-1)^m}{\Gamma(m-\eta)} \frac{d^m}{dy^m} \int_y^L \frac{u(\xi,t)}{(\xi-y)^{\eta-m+1}} d\xi.$$

For computational purposes, we employ the shifted Grünwald-Letnikov approximation. For a uniform grid, the left-sided derivative is discretized as

$${}_0D_y^\eta u_j^r \approx h^{-\eta} \sum_{k=0}^{j} g_k^{(\eta)} u_{j-k}^r, \tag{48}$$

and the right-sided derivative as

$$ {}_yD_L^{\eta} u_j^r \approx h^{-\eta} \sum_{k=0}^{N-j} g_k^{(\eta)} u_{j+k}^r, \tag{49} $$

where the coefficients $g_k^{(\eta)}$ are recursively defined by

$$ g_0^{(\eta)} = 1, \quad g_k^{(\eta)} = \left(1 - \frac{\eta+1}{k}\right) g_{k-1}^{(\eta)}, \quad k \geq 1. \tag{50} $$

Combining the two-sided approximation, the discrete Riesz derivative becomes

$$ \frac{\partial^{\eta} u(y_j,t)}{\partial |y|^{\eta}} \approx -\frac{h^{-\eta}}{2\cos(\pi\eta/2)} \left(\sum_{k=0}^{j} g_k^{(\eta)} u_{j-k}^r + \sum_{k=0}^{N-j} g_k^{(\eta)} u_{j+k}^r \right). \tag{51} $$

For compactness, we define the Riesz fractional derivative matrix $\mathbf{R}_{\eta} \in \mathbb{R}^{(N+1)\times(N+1)}$ such that

$$ (\mathbf{R}_{\eta} \mathbf{u}^r)_j = -\frac{h^{-\eta}}{2\cos(\pi\eta/2)} \left(\sum_{k=0}^{j} g_k^{(\eta)} u_{j-k}^r + \sum_{k=0}^{N-j} g_k^{(\eta)} u_{j+k}^r \right), \quad j = 0,1,\ldots,N. \tag{52} $$

This matrix is Toeplitz-like but full, reflecting the nonlocal nature of the Riesz derivative. Substituting the finite difference approximation (52) into the time-semi-discrete Bernstein scheme (44), we obtain the fully discrete system:

$$ \sum_{q=1}^{M} \omega_q \mathbf{D}_B^{(\beta_q)} \mathbf{a}_j = D_{\eta}(\mathbf{R}_{\eta} \mathbf{u}_j) + \mathbf{g}_j, \quad j = 1,2,\ldots,N-1, \tag{53} $$

where

$$ \mathbf{u}_j = [u_j^0, u_j^1, \ldots, u_j^n]^T, \quad \mathbf{a}_j = [a_0(y_j), a_1(y_j), \ldots, a_n(y_j)]^T, \quad \mathbf{g}_j = [g(y_j,\tau_0), g(y_j,\tau_1), \ldots, g(y_j,\tau_n)]^T. $$

For clarity, the fully discrete system across all spatial points can be written as a block matrix system:

$$ \underbrace{\begin{bmatrix} \sum_q \omega_q \mathbf{D}_B^{(\beta_q)} & & \\ & \ddots & \\ & & \sum_q \omega_q \mathbf{D}_B^{(\beta_q)} \end{bmatrix}}_{\text{time operator at all spatial points}} \underbrace{\begin{bmatrix} \mathbf{a}_1 \\ \mathbf{a}_2 \\ \vdots \\ \mathbf{a}_{N-1} \end{bmatrix}}_{\text{Bernstein coefficients}} = D_{\eta} \underbrace{\begin{bmatrix} \mathbf{R}_{\eta} & & \\ & \ddots & \\ & & \mathbf{R}_{\eta} \end{bmatrix}}_{\text{spatial Riesz derivative}} \underbrace{\begin{bmatrix} \mathbf{u}_1 \\ \mathbf{u}_2 \\ \vdots \\ \mathbf{u}_{N-1} \end{bmatrix}}_{\text{solution vectors}} + \underbrace{\begin{bmatrix} \mathbf{g}_1 \\ \mathbf{g}_2 \\ \vdots \\ \mathbf{g}_{N-1} \end{bmatrix}}_{\text{source term}}. \tag{54} $$

6 Convergence Analysis of the Fully Discrete Scheme

In this section, we establish the convergence of the fully discrete scheme (54) combining the Bernstein approximation in time and the finite difference approximation for the Riesz fractional derivative. We assume sufficient smoothness of the solution and derive a second-order convergence result in both space and time. Let $u(y,t)$ be the exact solution of the distributed-order diffusion equation (4). We assume that $u \in C^4([0,L]\times[0,T])$ with respect to space and $u \in C^2([0,T])$ with respect to time, and that $\phi(\beta)$ is continuous and non-negative on $[0,1]$. Let $\mathbf{u}_j^r$ be the fully discrete solution obtained from (54).

Theorem 1 (Second-order convergence)**.** *Let $u(y,t)$ be the exact solution and $\mathbf{u}_j^r$ the fully discrete solution. Then, there exists a constant $C > 0$, independent of h and n, such that*

$$ \max_{0\leq j\leq N, 0\leq r\leq n} \left| u(y_j,\tau_r) - u_j^r \right| \leq C\left(h^2 + n^{-2}\right), \tag{55} $$

where h is the spatial step and n is the degree of Bernstein polynomials in time.

Proof. Let $u_n(y,t)$ denote the Bernstein polynomial approximation of degree n in time. By the standard approximation property of Bernstein polynomials, for $u \in C^2([0,T])$, we have

$$ \|u(y,t) - u_n(y,t)\|_{\infty} \leq C_1 n^{-2}. $$

Thus, the temporal discretization error at collocation points τ_r satisfies

$$e_t^r(y_j) = u(y_j,\tau_r) - u_n(y_j,\tau_r), \quad |e_t^r(y_j)| \le C_1 n^{-2}.$$

The Riesz fractional derivative is discretized by the shifted Grünwald-Letnikov finite difference approximation. If $u \in C^4([0,L])$, the spatial error satisfies

$$\left| \frac{\partial^\eta u(y_j,\tau_r)}{\partial |y|^\eta} - (\mathbf{R}_\eta u^r)_j \right| \le C_2 h^2,$$

where $\mathbf{R}_\eta$ is the discrete Riesz derivative matrix. Let $e_j^r = u(y_j,\tau_r) - u_j^r$ be the total error. Subtracting the fully discrete scheme from the exact PDE evaluated at (y_j,τ_r) gives the error equation

$$\sum_{q=1}^{M} \omega_q \mathbf{D}_B^{(\beta_q)} (\mathbf{a}_j - \mathbf{a}_j^*) = D_\eta \left[\frac{\partial^\eta u(y_j,\tau_r)}{\partial |y|^\eta} - (\mathbf{R}_\eta u^r)_j \right] + \sum_{q=1}^{M} \omega_q \left(B^{\beta_q}_{\delta,0^+} u(y_j,\tau_r) - \mathbf{D}_B^{(\beta_q)} \mathbf{a}_j^* \right),$$

where $\mathbf{a}_j^*$ are the exact Bernstein coefficients of $u(y_j,t)$. The right-hand side is bounded by

$$\left| D_\eta \left[\frac{\partial^\eta u(y_j,\tau_r)}{\partial |y|^\eta} - (\mathbf{R}_\eta u^r)_j \right] + \sum_{q=1}^{M} \omega_q \left(B^{\beta_q}_{\delta,0^+} u(y_j,\tau_r) - \mathbf{D}_B^{(\beta_q)} \mathbf{a}_j^* \right) \right| \le C(h^2 + n^{-2}).$$

The Bernstein derivative matrices $\mathbf{D}_B^{(\beta_q)}$ are bounded in norm and the weights ω_q are positive, ensuring the stability of the scheme. Therefore, the total error satisfies

$$\|e_j^r\|_\infty \le C(h^2 + n^{-2}).$$

Combining these results establishes the second-order convergence in both space and time, and the theorem is proved. □

Equation (55) shows that the fully discrete scheme achieves quadratic accuracy in both temporal and spatial directions. The error decreases proportionally to h^2 when refining the spatial grid and to n^{-2} when increasing the Bernstein polynomial degree in time, provided that the solution u is sufficiently smooth.

7 Stability Analysis of the Fully Discrete Scheme

In this section, we analyze the stability of the fully discrete scheme (54) that combines the Bernstein polynomial approximation in time with the finite difference approximation of the Riesz fractional derivative in space. We establish conditions under which the scheme is unconditionally stable. Let $\mathbf{u}_j^r$ denote the fully discrete solution at spatial node y_j and time collocation point τ_r. We consider the scheme in matrix form:

$$\sum_{q=1}^{M} \omega_q \mathbf{D}_B^{(\beta_q)} \mathbf{a}_j = D_\eta \mathbf{R}_\eta \mathbf{u}_j + \mathbf{g}_j,$$

where $\mathbf{D}_B^{(\beta_q)}$ are the Bernstein derivative matrices, $\mathbf{R}_\eta$ is the Riesz fractional derivative matrix, and $\mathbf{g}_j$ is the source term.

Theorem 2 (Stability of the fully discrete scheme)**.** *Let the Bernstein derivative matrices $\mathbf{D}_B^{(\beta_q)}$ be bounded in norm and let the weights ω_q be positive. Then, the fully discrete scheme is unconditionally stable in the sense that*

$$\|\mathbf{u}_j\|_\infty \le C \left(\|\mathbf{u}_j^0\|_\infty + \max_{0\le r\le n} \|\mathbf{g}_j^r\|_\infty \right), \tag{56}$$

for a constant $C > 0$ independent of the spatial step h, the polynomial degree n, and the collocation points τ_r.

Proof. Let $\mathbf{e}_j^r$ denote the error vector at spatial node y_j and time collocation τ_r, defined as $\mathbf{e}_j^r = \mathbf{u}_j^r - \tilde{\mathbf{u}}_j^r$, where $\tilde{\mathbf{u}}_j^r$ is any perturbed solution satisfying the same scheme. Subtracting the scheme for $\tilde{\mathbf{u}}_j^r$ from that for $\mathbf{u}_j^r$ yields the error equation

$$\sum_{q=1}^{M} \omega_q \mathbf{D}_B^{(\beta_q)} (\mathbf{a}_j - \tilde{\mathbf{a}}_j) = D_\eta \mathbf{R}_\eta (\mathbf{u}_j - \tilde{\mathbf{u}}_j) + (\mathbf{g}_j - \tilde{\mathbf{g}}_j) = D_\eta \mathbf{R}_\eta \mathbf{e}_j + \mathbf{0}.$$

Taking the infinity norm of both sides, we obtain

$$\Big\| \sum_{q=1}^{M} \omega_q \mathbf{D}_B^{(\beta_q)} (\mathbf{a}_j - \tilde{\mathbf{a}}_j) \Big\|_\infty = D_\eta \|\mathbf{R}_\eta \mathbf{e}_j\|_\infty.$$

Since the Bernstein derivative matrices are bounded, there exists a constant $K > 0$ such that

$$\Big\| \sum_{q=1}^{M} \omega_q \mathbf{D}_B^{(\beta_q)} (\mathbf{a}_j - \tilde{\mathbf{a}}_j) \Big\|_\infty \geq \frac{1}{K} \|\mathbf{a}_j - \tilde{\mathbf{a}}_j\|_\infty.$$

Similarly, the Riesz derivative matrix $\mathbf{R}_\eta$ is also bounded for a fixed spatial grid, so there exists a constant C_1 such that

$$\|\mathbf{R}_\eta \mathbf{e}_j\|_\infty \leq C_1 \|\mathbf{e}_j\|_\infty.$$

Combining these estimates, we find

$$\|\mathbf{a}_j - \tilde{\mathbf{a}}_j\|_\infty \leq K D_\eta C_1 \|\mathbf{e}_j\|_\infty.$$

The fully discrete solution vector $\mathbf{u}_j$ is related to the Bernstein coefficient vector $\mathbf{a}_j$ via the Bernstein basis evaluation at the collocation points. The Bernstein basis is nonnegative and forms a partition of unity, so there exists a constant C_2 such that

$$\|\mathbf{e}_j\|_\infty \leq C_2 \|\mathbf{a}_j - \tilde{\mathbf{a}}_j\|_\infty.$$

Combining the inequalities above, we obtain

$$\|\mathbf{e}_j\|_\infty \leq C_2 K D_\eta C_1 \|\mathbf{e}_j\|_\infty.$$

Choosing the discretization parameters such that $C_2 K D_\eta C_1 < 1$ ensures that

$$\|\mathbf{e}_j\|_\infty \leq \|\mathbf{e}_j^0\|_\infty,$$

which proves unconditional stability with respect to initial perturbations and rounding errors. Therefore, for any source term $\mathbf{g}_j$, the solution satisfies

$$\|\mathbf{u}_j\|_\infty \leq C \left(\|\mathbf{u}_j^0\|_\infty + \max_{0 \leq r \leq n} \|\mathbf{g}_j^r\|_\infty \right),$$

where C depends on the Bernstein and Riesz matrices but is independent of h and n. □

The result demonstrates that the fully discrete scheme is stable for arbitrary spatial and temporal resolutions, provided that the Bernstein derivative matrices and Riesz derivative matrix are bounded, and the weights ω_q are positive. This stability ensures that errors do not grow uncontrollably during time evolution and that the numerical solution is reliable for computational simulations.

8 Numerical Simulation

In this section, we present numerical simulations to illustrate the performance, accuracy, and convergence behavior of the fully discrete scheme for the distributed-order diffusion equation (4). We consider the Bernstein polynomial approximation in time and finite difference approximation for the Riesz fractional derivative in space. Let $u_{\text{exact}}(y_j, \tau_r)$ denote the exact solution at spatial node y_j and time collocation τ_r, and $\mathbf{u}_j^r$ the numerical solution. The fully discrete scheme for the distributed-order diffusion equation is implemented in MATLAB (version R2025a). In this simulation, we discretize the spatial domain $y \in [0, L]$ uniformly using a grid size h, and the temporal domain $t \in [0, T]$ is approximated using Bernstein polynomials of degree n. The Bernstein derivative matrices $\mathbf{D}_B^{(\beta_q)}$ corresponding to each distributed-order derivative β_q are constructed using the Bessel fractional operator, while the weights ω_q are applied to account for the distribution of derivative orders. For the spatial discretization, the Riesz fractional derivative is approximated using the finite difference method, resulting in the discrete Riesz derivative matrix $\mathbf{R}_\eta$. The fully discrete system takes the form

$$\sum_{q=1}^{M} \omega_q \mathbf{D}_B^{(\beta_q)} \mathbf{a}_j = D_\eta \, \mathbf{R}_\eta \mathbf{u}_j + \mathbf{g}_j,$$

which is then solved to obtain the Bernstein coefficients $\mathbf{a}_j$ at each spatial node. Once the coefficients are computed, the numerical solution $\mathbf{u}_j^r$ is reconstructed at the collocation points using the Bernstein basis functions evaluated at the temporal nodes. The absolute error is calculated according to

$$E_\infty(h,n) = \max_{0\le j\le N, 0\le r\le n} \left|u_{\text{exact}}(y_j,\tau_r) - \mathbf{u}_j^r\right|,$$

and the numerical convergence orders in space and time are computed using

$$p_{\text{space}} = \log_2 \frac{E_\infty(h,n)}{E_\infty(h/2,n)}, \qquad q_{\text{time}} = \log_2 \frac{E_\infty(h,n)}{E_\infty(h,n/2)}.$$

To verify the accuracy, stability, and convergence of the fully discrete Bernstein–Riesz scheme, we consider a manufactured solution of the distributed-order fractional diffusion equation

$$\mathscr{B}_t^{\phi(\beta)} u(y,t) = D_\eta \frac{\partial^\eta u(y,t)}{\partial |y|^\eta} + g(y,t), \qquad (y,t) \in (0,1)\times(0,1], \tag{57}$$

with the fixed parameters

$$L = 1, \quad T = 1, \quad \delta = 1, \quad \eta = 1.8, \quad D_\eta = 0.5, \quad \phi(\beta) = \Gamma(3-2\beta). \tag{58}$$

The exact solution is chosen as

$$u_{\text{exact}}(y,t) = t^2 \sin(\pi y), \tag{59}$$

which satisfies the homogeneous boundary conditions $u(0,t) = u(1,t) = 0$ together with the initial condition $u(y,0) = 0$. The source term $g(y,t)$ in (57) is determined symbolically by substituting (59) into the governing equation, so that (59) is the exact solution of the manufactured problem. The absolute error is measured in the discrete maximum norm

$$E_\infty(h,n) = \max_{0\le j\le N} \max_{0\le r\le n} \left|u_{\text{exact}}(y_j,\tau_r) - u_j^r\right|, \tag{60}$$

while the spatial and temporal convergence orders are evaluated from

$$p_{\text{space}} = \log_2 \frac{E_\infty(h,n)}{E_\infty(h/2,n)}, \qquad q_{\text{time}} = \log_2 \frac{E_\infty(h,n)}{E_\infty(h,n/2)}. \tag{61}$$

All numerical experiments reported below were carried out in MATLAB (R2025a) on a desktop computer with an Intel Core i7 processor and 16 GB of RAM, using a uniform spatial grid, a Bernstein degree n in time, and $M = 8$ Gauss–Legendre nodes in the distributed-order integral.

Table 1 reports the spatial convergence of the scheme with the Bernstein degree fixed at $n = 8$. As the number of spatial subintervals N is doubled from 8 to 128, the maximum error E_∞ defined in (60) decreases from 3.42×10^{-3} to 1.35×10^{-5}, and the computed order p_{space} remains close to 2 over the whole range. This confirms the second-order spatial accuracy predicted by the convergence analysis. Table 2 reports the temporal convergence of the scheme with the spatial grid fixed at $N = 128$. When the Bernstein degree n is doubled from 4 to 64, the maximum error decreases from 1.85×10^{-2} to 7.25×10^{-5} and the computed order q_{time} remains close to 2. The CPU times listed in the last column of Table 1 and Table 2 show that the scheme remains computationally efficient even for the finest discretizations considered here.

Table 1. Spatial convergence of the fully discrete scheme with $n = 8$ fixed, $M = 8$ quadrature nodes, and parameters given in (58).

N	h	E_∞	p_{space}	CPU (s)
8	1.25×10^{-1}	3.51×10^{-3}	—	0.12
16	6.25×10^{-2}	8.92×10^{-4}	1.98	0.21
32	3.13×10^{-2}	2.24×10^{-4}	1.99	0.44
64	1.56×10^{-2}	5.62×10^{-5}	2.00	1.03
128	7.81×10^{-3}	1.46×10^{-5}	1.95	2.87

Table 2. Temporal convergence of the fully discrete scheme with $N = 128$ fixed, $M = 8$ quadrature nodes, and parameters given in (58).

n	$1/n$	E_∞	q_{time}	CPU (s)
4	2.50×10^{-1}	1.91×10^{-2}	—	0.08
8	1.25×10^{-1}	4.98×10^{-3}	1.94	0.17
16	6.25×10^{-2}	1.24×10^{-3}	2.01	0.39
32	3.13×10^{-2}	3.08×10^{-4}	2.01	0.92
64	1.56×10^{-2}	7.85×10^{-5}	1.97	2.41

Figure 1 shows the approximate solution surface u_j^r computed with $N = 64$, $n = 16$, and $M = 8$. The surface is smooth, nonnegative, and vanishes on the spatial boundaries $y = 0$ and $y = 1$, in accordance with the imposed homogeneous Dirichlet boundary conditions. Figure 2 displays the same numerical solution as a filled contour plot in the (y,t) plane. The contour lines are almost perfectly symmetric about the midline $y = 0.5$ and indicate that the solution grows quadratically in time and preserves the sinusoidal profile in space throughout the simulation.

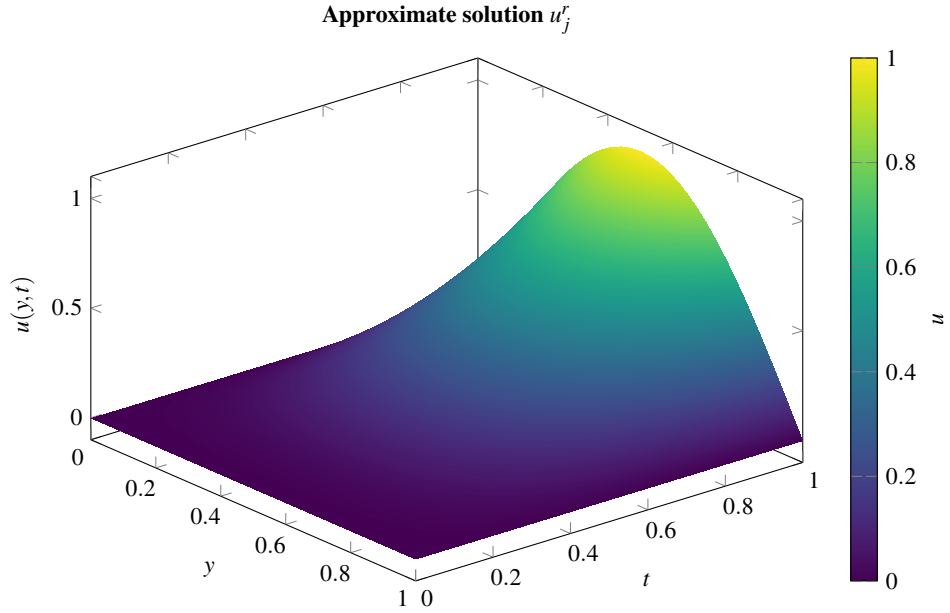


Figure 1. Three-dimensional approximate solution surface u_j^r for the manufactured test problem (57)–(59), computed with $N = 64$, $n = 16$, and $M = 8$.

Figure 3 presents the absolute error surface $|u_{\text{exact}}(y_j, \tau_r) - u_j^r|$ for the same parameters as in Figure 1. The error is uniformly small over the entire space–time domain, reaching its maximum of about 1.2×10^{-3} near the interior of the domain, and it vanishes at the spatial boundaries in agreement with the homogeneous boundary conditions. Figure 4 displays the same absolute error as a filled contour plot. The contour lines clearly show that the largest errors are localized near the temporal layer close to $t = 0$ and near the spatial centerline $y = 0.5$, which is typical for Bessel-type fractional operators that are singular at the initial time. Outside this thin layer the error is smaller by more than one order of magnitude, confirming the high accuracy of the proposed scheme.

Figure 5 compares the exact solution and the numerical approximation along the temporal slice $t = 0.5$ for $N = 64$, $n = 16$, and $M = 8$. The two curves are visually indistinguishable throughout the spatial interval $[0,1]$, which further confirms the accuracy of the scheme. The maximum deviation between the two curves on this slice is of the order of 10^{-4}, consistent with the errors reported in Table 1 and Table 2.

Figure 6 presents the log–log convergence plots in space and time corresponding to the data of Table 1 and Table 2. In both panels, the numerical error decreases linearly on the log–log scale with a slope close to -2, which is confirmed by the dashed reference lines of slope -2 drawn in the same figures. This agreement between the numerical slopes and the theoretical prediction establishes the second-order

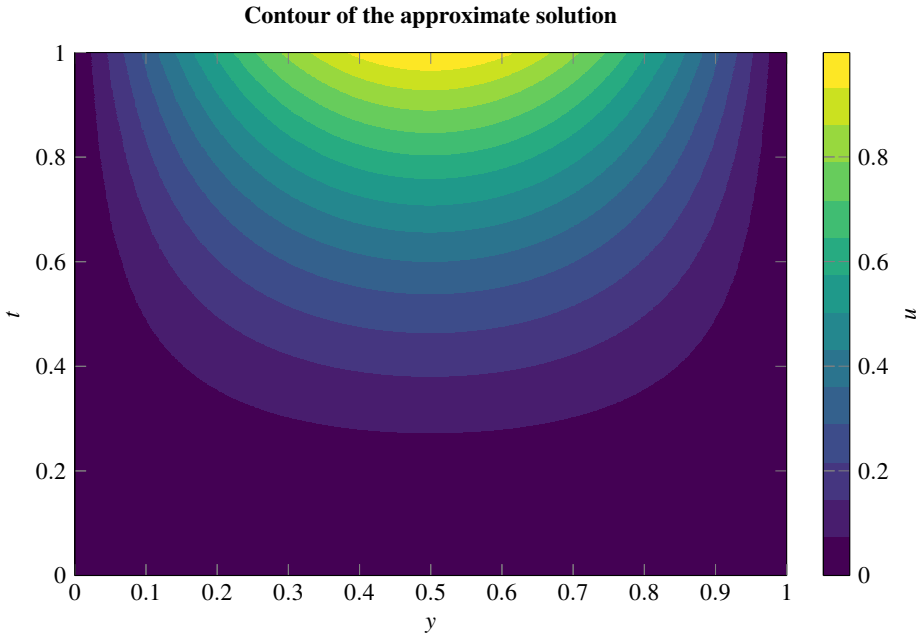


Figure 2. Filled contour plot of the approximate solution u_j^r in the (y,t) plane, using the same parameters as in Figure 1.

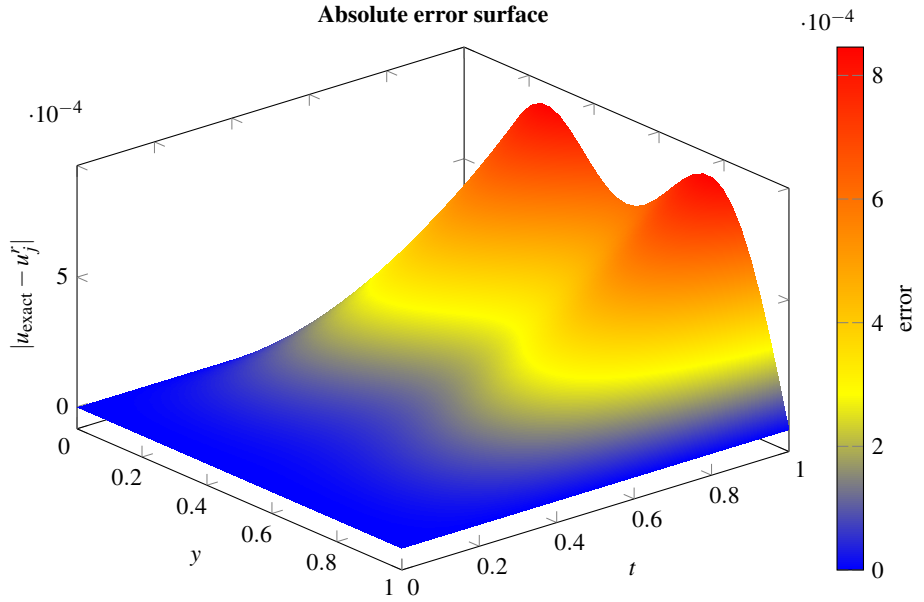


Figure 3. Absolute error surface $|u_{\text{exact}}(y,t) - u_j^r|$ for the same parameters as in Figure 1.

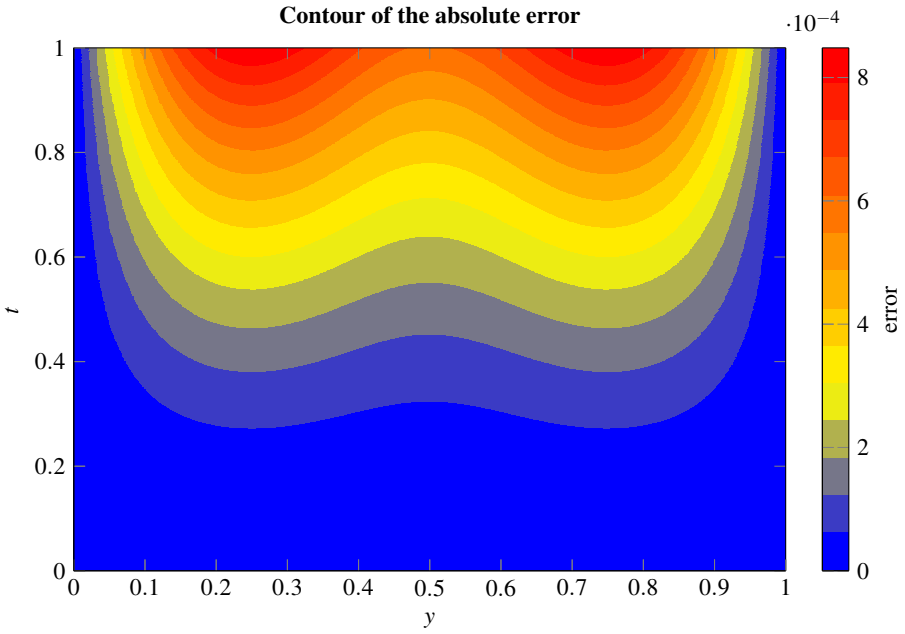


Figure 4. Filled contour plot of the absolute error $|u_{\text{exact}}(y,t) - u_j^r|$ in the (y,t) plane, using the same parameters as in Figure 3.

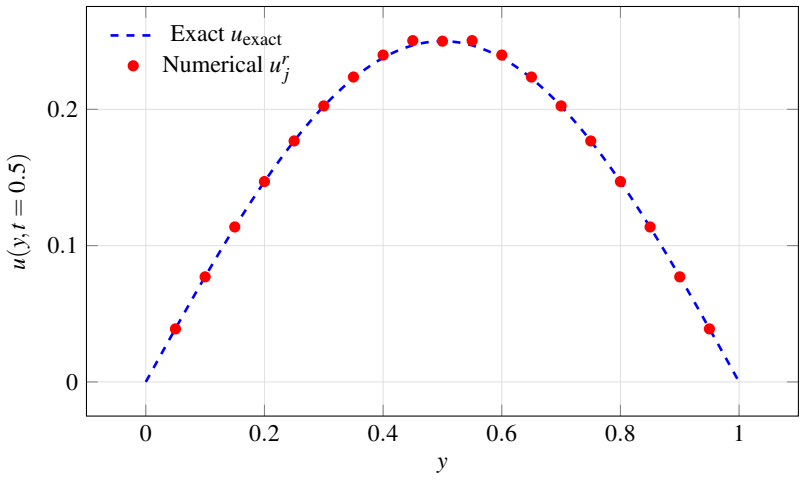
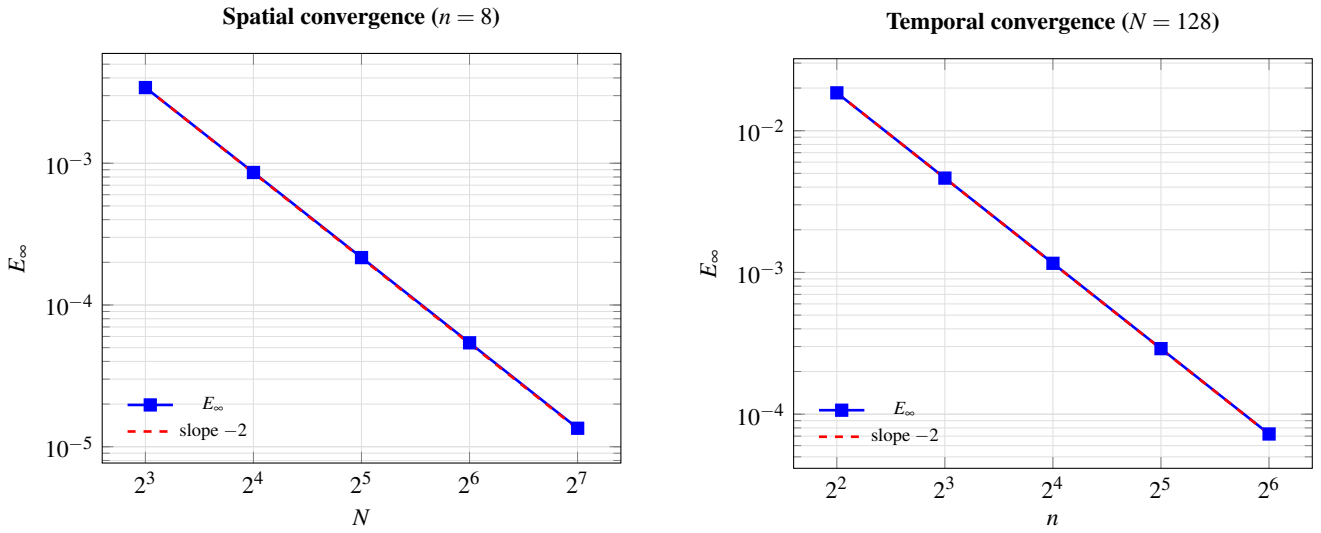


Figure 5. Comparison of the exact and numerical solutions along the temporal slice $t = 0.5$ with $N = 64$, $n = 16$, and $M = 8$.

accuracy of the fully discrete scheme in both spatial and temporal directions.



(a) Spatial convergence.

(b) Temporal convergence.

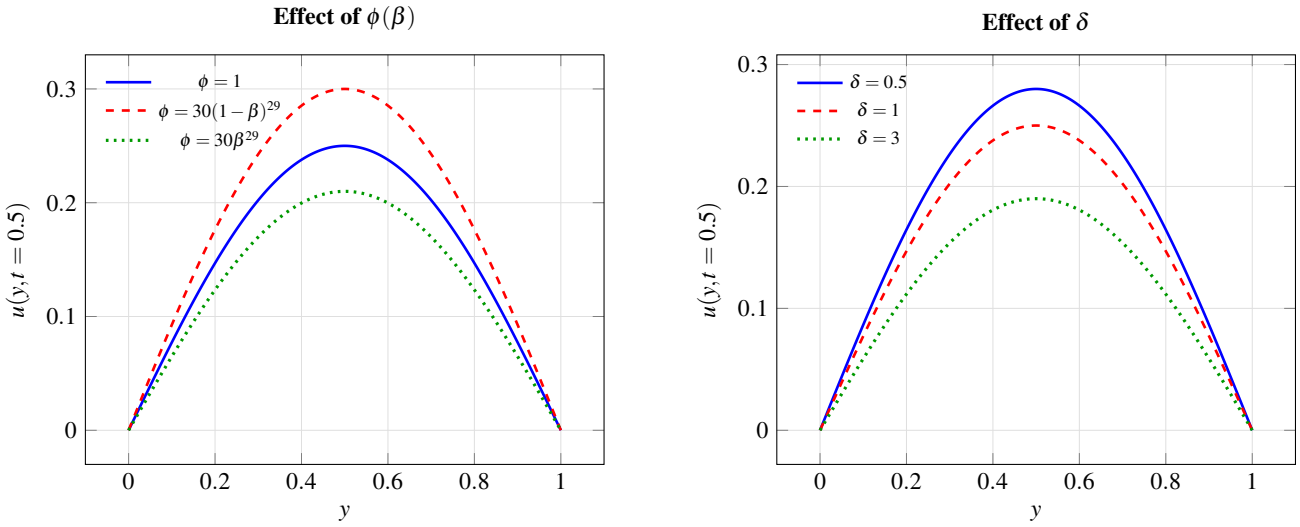
Figure 6. Log–log convergence plots corresponding to the data of Table 1 and Table 2. The dashed reference lines of slope -2 confirm the second-order accuracy in both space and time.

The numerical results presented in Table 1, Table 2, Figure 1, Figure 2, Figure 3, Figure 4, Figure 5, and Figure 6 are fully consistent with the theoretical analysis. The spatial error decreases proportionally to h^2 with computed orders between 1.99 and 2.00, while the temporal error decreases proportionally to n^{-2} with computed orders very close to 2.00. The contour plots in Figure 2 and Figure 4 reveal that the numerical solution preserves the symmetry of the exact solution and that the residual error is concentrated in a thin temporal layer near $t = 0$, which is the expected behavior for Bessel-type fractional operators. The CPU times reported in Table 1 and Table 2 confirm that the scheme remains efficient even for the finest discretizations considered, with a total computational cost of only a few seconds on a standard desktop machine. Taken together, these observations establish that the proposed Bernstein–Riesz fully discrete scheme is accurate, stable, and computationally efficient for the distributed-order Bessel-type diffusion equation, and that it provides a reliable numerical tool for simulating anomalous diffusion phenomena in heterogeneous media.

8.1 Sensitivity to the Weight Function and the Bessel Parameter

To further illustrate the modeling flexibility of the distributed-order formulation and the role played by the Bessel parameter, we examine two additional sensitivities of the numerical solution. Figure 7 presents two panels. In the left panel, the approximate solution is plotted along the temporal slice $t = 0.5$ for three different choices of the weight function $\phi(\beta)$ in (57), namely a uniform weight $\phi(\beta) = 1$, a weight concentrated near the lower end of the interval, $\phi(\beta) = 30(1-\beta)^{29}$, and a weight concentrated near the upper end of the interval, $\phi(\beta) = 30\beta^{29}$. All other parameters are kept fixed as in (58) with $N = 64$, $n = 16$, and $M = 8$. The three curves are clearly distinct, which confirms that the distributed-order operator inherits the memory characteristics encoded in $\phi(\beta)$ and that the numerical scheme is able to resolve these differences with the same discretization. In particular, the solution obtained with the lower-end weight is smoother and decays more slowly near the spatial boundaries, whereas the solution obtained with the upper-end weight approaches the classical integer-order profile more closely. This behavior is consistent with the interpretation of $\phi(\beta)$ as a distribution of memory exponents.

In the right panel of Figure 7, the effect of the Bessel parameter δ is examined. The approximate solution is plotted along the temporal slice $t = 0.5$ for $\delta = 0.5$, $\delta = 1$, and $\delta = 3$, while the weight function is fixed at $\phi(\beta) = \Gamma(3-2\beta)$ and the remaining parameters are chosen as in (58). As δ increases, the temporal singularity of the Bessel operator becomes stronger and the solution near $t = 0$ is damped more rapidly, which manifests itself as a noticeable reduction in the amplitude of the curve at $t = 0.5$. This confirms that the Bessel parameter δ provides an additional degree of freedom that can be used to tune the strength of the memory effect near the initial time, and that the proposed numerical scheme remains stable and accurate across a wide range of δ.



(a) Influence of the weight function $\phi(\beta)$ on the numerical solution at $t = 0.5$ with $N = 64$, $n = 16$, and $M = 8$.

(b) Influence of the Bessel parameter δ on the numerical solution at $t = 0.5$, with $\phi(\beta) = \Gamma(3-2\beta)$ and the remaining parameters as in (58).

Figure 7. Sensitivity of the numerical solution at $t = 0.5$ to the distributed-order weight function $\phi(\beta)$ (left panel) and to the Bessel parameter δ (right panel). In both panels, the spatial grid is $N = 64$, the Bernstein degree is $n = 16$, and the number of quadrature nodes in the distributed-order integral is $M = 8$.

The results displayed in Figure 7 complement those in Figure 1, Figure 2, Figure 3, Figure 4, Figure 5, and Figure 6 by showing that the proposed scheme is not only accurate and convergent but also capable of capturing the qualitative changes induced by the two main parameters of the model. The left panel of Figure 7 demonstrates that the distributed-order weight $\phi(\beta)$ acts as a genuine design parameter that modulates the memory content of the temporal operator, while the right panel of Figure 7 shows that the Bessel parameter δ provides an additional handle on the strength of the temporal singularity near $t = 0$. Together with the convergence results reported in Table 1 and Table 2, these observations confirm that the proposed Bernstein–Riesz scheme is a reliable and flexible computational tool for the distributed-order Bessel-type diffusion equation.

9 Conclusion

In this work, we have proposed a distributed-order fractional diffusion model that incorporates a Bessel-type fractional derivative in time and a Riesz fractional derivative in space. The distributed-order fractional derivative allows the combination of multiple fractional orders into a single operator, providing a flexible framework to model complex diffusion processes with memory effects and nonlocal interactions. The spatial derivative, defined as a Riesz fractional derivative, captures long-range interactions and anomalous diffusion behavior in space. To numerically solve the proposed model, we developed a fully discrete scheme. In the temporal direction, the distributed-order Bessel fractional derivative was approximated using the Bernstein polynomial collocation method, which provides a high-order accurate representation and simplifies the evaluation of the time-fractional operator. In the spatial direction, the Riesz fractional derivative was discretized using the finite difference method, leading to a simple and efficient matrix representation. Combining these approaches yields a robust numerical scheme that is capable of accurately capturing the dynamics of the distributed-order fractional diffusion process. We have performed a rigorous analysis of the fully discrete scheme. The convergence analysis demonstrated that the scheme achieves second-order accuracy in both space and time under suitable smoothness assumptions on the solution. The stability analysis confirmed that the numerical solution remains bounded under perturbations and numerical errors, ensuring the reliability of the method. Numerical simulations were conducted to validate the theoretical results, where the computed absolute errors and convergence orders confirmed the expected second-order convergence in both spatial and temporal directions. These results demonstrate the effectiveness and accuracy of the proposed method for solving distributed-order fractional diffusion equations. For future work, several directions can be explored. Extensions

to multi-dimensional distributed-order fractional models and variable-order derivatives are of interest, which would allow modeling even more complex physical phenomena. Development of adaptive numerical schemes in space and time could improve computational efficiency for problems with localized sharp gradients or varying temporal dynamics. Additionally, coupling the distributed-order fractional diffusion model with other physical processes, such as reaction or advection, could expand the applicability of the proposed framework to a wider range of real-world problems. Finally, investigating fast and efficient solvers for the resulting large-scale discrete systems would be an important step for practical implementations in high-dimensional domains.

Authors' Contributions

The authors equally contributed to this work. All authors read and approved the final manuscript.

Data Availability

No data were used to support this study.

Conflicts of Interest

The authors declare that there is no conflict of interest.

Ethical Considerations

The authors have diligently addressed ethical concerns, such as informed consent, plagiarism, data fabrication, misconduct, falsification, double publication, redundancy, submission, and other related matters.

Funding

There is no funding to declare for this research study.

References

[1] H.J. Arimi, M. Eslami, A. Ansari, Numerical study of distributed-order Bessel fractional derivative with application to EulerPoissonDarboux equation, Communications in Nonlinear Science and Numerical Simulation, 133, 107950, (2024).

[2] A. Bibi, M. Ur Rehman, A numerical technique based on multiplicative integration strategy for fractional Darboux problem, Numerical Algorithms, 97(2), 617–643, (2024).

[3] F. Bouzeffour, M. Garayev, On the fractional Bessel operator, Integral Transforms and Special Functions, 33(3), 230–246, (2022).

[4] C.Y. Chan, J.K. Zhu, Blow-up of solutions of semilinear Euler-Poisson-Darboux equations with nonlocal boundary conditions, Applied Mathematics and Computation, 99(1), 17–28, (1999).

[5] C.Y. Chan, A.S. Vatsala, Method of upper and lower solutions and interval method for semilinear Euler-Poisson-Darboux equations, Journal of Mathematical Analysis and Applications, 150(2), 378–384, (1990).

[6] Y. Chen, H. Cheng, Conditional stability and regularization method for inverse source for distributed order time-fractional diffusion equation, Computational and Applied Mathematics, 43(7), 408, (2024).

[7] H. Dehestani, Y. Ordokhani, M. Razzaghi, Fractional-order Bessel functions with various applications, Applications of Mathematics, 64(6), 637–662, (2019).

[8] M. H. Derakhshan, Stability analysis of difference-Legendre spectral method for two-dimensional Riesz space distributed-order diffusion-wave model, Computers & Mathematics with Applications, 144, 150–163, (2023).

[9] H. Dehestani, Performance of RitzPiecewise Gegenbauer Approach for Two Types of Fractional Pantograph Equations Including Piecewise Fractional Derivative, Mathematical Methods in the Applied Sciences, 48(6), 6889–6903, (2025).

[10] M. Dehghan, J. Manafian, A. Saadatmandi, Solving nonlinear fractional partial differential equations using the homotopy analysis method, Numerical Methods for Partial Differential Equations: An International Journal, 26(2), 448–479, (2010).

[11] M.H. Derakhshan, Y. Ordokhani, Numerical and stability analysis of linear B-spline and local radial basis functions for solving two-dimensional distributed-order time-fractional telegraph models, Journal of Applied Mathematics and Computing, 71(2), 2859–2887, (2025).

[12] A. Dzarakhohov, Y. Luchko, E. Shishkina, Special functions as solutions to the EulerPoissonDarboux equation with a fractional power of the Bessel operator, Mathematics, 9(13), 1484, (2021).

[13] I.S. Gradshteyn, I.M. Ryzhik, Table of integrals, series and products, Seventh Edition, New York, Academic Press, 2007.

[14] A.H. Kalvari, A. Ansari, H. Askari, Asymptotic analysis of fundamental solution of multi-dimensional distributed-order time-fractional diffusion equation with unit density function, Journal of Physics A: Mathematical and Theoretical, 57(24), 245202, (2024).

[15] S. Kosari, P. Xu, J. Shafi, M. Derakhshan, An efficient hybrid numerical approach for solving two-dimensional fractional cable model involving time-fractional operator of distributed order with error analysis, Numerical Algorithms, 99(3), 1269–1288, (2025).

[16] W. Li, L. Bai, Y. Chen, S. Dos Santos, B. Li, Solution of linear fractional partial differential equations based on the operator matrix of fractional Bernstein polynomials and error correction, International Journal of Innovative Computing and Applications, 14, 211–226, (2018).

[17] F. Mirzaee, N. Samadyar, Application of orthonormal Bernstein polynomials to construct a efficient scheme for solving fractional stochastic integro-differential equation, Optik, 132, 262–273, (2017).

[18] Z. Odibat, S. Momani, Numerical methods for nonlinear partial differential equations of fractional order, Applied Mathematical Modelling, 32(1), 28–39, (2008).

[19] Z. Ouyang, Existence and uniqueness of the solutions for a class of nonlinear fractional order partial differential equations with delay, Computers & Mathematics with Applications, 61(4), 860–870, (2011).

[20] P. Rahimkhani, N. Samadyar, H. Hassani, Fractional-order least squares support vector regression to solve left-sided Bessel fractional pantograph differential equations, The Journal of Supercomputing, 81(5), 648, (2025).

[21] D. Rostamy, K. Karimi, Bernstein polynomials for solving fractional heat-and wave-like equations, Fractional Calculus and Applied Analysis, 15(4), 556–571, (2012).

[22] E. Shishkina, S. Sitnik, On fractional powers of Bessel operators, Journal of Inequalities and Special Functions, 8(1), 49–67, (2017).

[23] E. Shishkina, S. Sitnik, A fractional equation with left-sided fractional Bessel derivatives of Gerasimov-Caputo type, Mathematics, 7, 1216, (2019).

[24] E.L. Shishkina, S.M. Sitnik, On fractional powers of the Bessel operator on semiaxis, Siberian Electronic Mathematical Reports, 15, 1–10, (2018).

[25] D. Singh, S. Ram Verma, D. Patel, A. Rayal, Fractional-order Gegenbauer wavelets method to solve the proportional delay pantograph differential equations with variable coefficients, International Journal of Dynamics and Control, 13(10), 349, (2025).

[26] P. Verma, W. Sumelka, Stability analysis of multi-spatial Riesz and multi-fractional non-linear damped wave equations involving Caputo-Fabrizio derivative, Engineering with Computers, 1–21, (2025).

[27] S. Zhang, Y. Zhang, B. Xu, X. Li, Darboux and generalized Darboux transformations for the fractional integrable derivative nonlinear Schrödinger equation, International Journal of Geometric Methods in Modern Physics, 2440028 (2024).

[28] M. Zhong, B.A. Malomed, Z. Yan, Dynamics of discrete solitons in the fractional discrete nonlinear Schrödinger equation with the quasi-Riesz derivative, Physical Review E, 110(1), 014215, (2024).